RSC Advances

ROYAL SOCIETY OF CHEMISTRY

www.rsc.org/advances

Journal Name

RSCPublishing

ARTICLE

Electrostatically Driven Self-Assembly of CdTe Nanoparticles with Organic Chromophores Probed via Ham Effect

Arun Gopi[a,b], Asarikal Vindhyasarumi[a] and Karuvath Yoosaf [a,b] *

Cite this: DOI: 10.1039/x0xx00000x

Received ooth January 2012,
Accepted ooth January 2012

DOI: 10.1039/x0xx00000x

www.rsc.org/

Abstract: We demonstrate that polarity influence on the pyrene fluorescence band ratios (I_3/I_1) termed as Ham effect can be effectively utilized to study the electrostatic interaction of CdTe nanoparticles (ζ = - 46 mV) with oppositely charged organic molecule, pyrenemethylamine hydrochloride (PMAH). When compared to water, the less polar nature of QD's surface resulted in an increase in I_3/I_1 peak ratio of PMAH (0.34 to 0.54) when brought in close proximity. The lowering of the asymmetric stretching frequencies of the carboxylate groups of thioglycolic acid (1570 cm^{-1} to ~1550 cm^{-1}) and a drop in zeta potential of the nanoparticle from -46 mV to -8 mV indicates the interaction of the PMAH with the nanoparticles. Control experiments with capping ligands, QDs having different surface charges (-46, -39, -35, -31, -20 and +21 mV) and negatively charged pyrene molecules invariably supports the role of nanoparticles and its surface charge. The combined effects of charge neutralization and hydrophobicity increase lead to the organization of QDs into 2D sheet like superstructures preserving their initial individuality.

Introduction

Organic-inorganic nanohybrids are of prime current research interest as they provide materials with newer properties that are distinct from their individual components. Recent literature reports show that these materials have got immense potential in the upcoming opto-electronic technologies[1, 2] such as organic photovoltaics,[3, 4] light emitting devices[5, 6] and in many bio medicinal applications.[1, 7-9] It is well understood that, in addition to size and composition, their performance is greatly affected by their organization at the interface. Based on the origin, mainly there are two types of organic-inorganic hybrids;[10] in class I, organic and inorganic components are assembled with weak bonds whereas class II materials are formed through strong covalent interactions. Self-assembly serve as a key process for the formation of class I type materials and offers more flexibility of design and post synthetic modifications. It is clear that various noncovalent interactions and environmental conditions play a crucial role in their formation and an in-depth understanding is required. Among the various, systems based on electrostatic interactions are highly appealing due to their simplicity of design and its precise complementarity. They have been extensively used in both material[11-13] and bio applications.[14, 15] However, a deeper understanding on such non covalent interactions in nanohybrids are limited mainly because of the complexity and diversity of the nanostructure especially at the interfaces. Compared to other conventional techniques fluorescence have the advantages of high sensitivity and ease of instrumentation. Nevertheless, their wide use is often limited by requirements of selective excitation wavelength or clear isosbestic point and a change in fluorescence intensity as a result of excited state energy or electron transfer processes.[16, 17]

It has been demonstrated that the relative intensity of vibronic features present in the electronic transition of certain poly-aromatic hydrocarbons such as pyrene are highly sensitive to the polarity of its immediate surroundings and is termed as Ham effect.[18] In 1982 Dong and Winnik introduced the concept of Py empirical scale to define polarity of solvents irrespective of their protic/aprotic nature.[19, 20] This has also been effectively utilized to study the various complex phenomena such as localization of fluorophores in micelles, polymer matrices,[21] organization dynamics of bio-membranes,[22] polarity of nanoparticle surface[23] and others.[24] Herein, we show that this methodology can be extended to study the electrostatic driven self-assembly, in water, of an inorganic nanomaterial with an organic counter part. Our studies also revealed that electrostatic interaction results in charge neutralization and diminishing of

repulsive forces between the nanocrystals that leads to formation of 2D sheet like superstructures.

To demonstrate this we have considered a simple system consisting of CdTe inorganic nanoparticles (CdTe QDs) and pyrene derivative as the organic molecule. In addition to the Ham effect, the other rationale for selection are (i) the surface charge of nanoparticles can easily be modulated by capping with appropriate ligands, (ii) negative and positive derivatized pyrenes are easily available (iii) the electrostatic attraction of oppositely charged materials would bring them close to each other (Scheme 1) and (iv) the emission profile of CdTe QDs and pyrene chromophore are well separated (Fig. 2) and hence independent monitoring of individual fluorescence signals are possible.

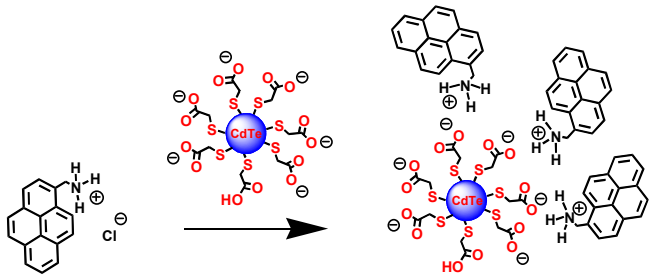

Scheme 1. Pictorial representation of electrostatic driven self-assembly.

Experimental Section

Materials and methods

Chemicals such as cadmium acetate dihydrate, cadmium chloride hydrate, tellurium powder, sodium tellurite, pyrene butyric acid (PBA), copper perchlorate hexahydrate, pyrenemethylamine hydrochloride (PMAH) and thioglycolic acid (TGA) were purchased from Ms. Sigma Aldrich. Hydroxylamine hydrochloride and cysteamine hydrochloride (CA) were acquired from Ms. Alfa Aeser. Sodium borohydride, sodium hydroxide and solvents such as methanol and acetone were obtained from Ms. Merck India Pvt. Ltd. All chemicals were used as received without further purification. Stock solutions were prepared in doubly distilled water and titration experiments were performed by adding aliquot amounts to a 3 mL (1 cm) quartz cuvette.

UV-visible absorption spectra were obtained using Shimadzu UV-2401PC and UV-2600 spectrophotometers. Emission spectra were collected using SPEX-Fluorolog F112X1 fluorimeter. The excitation wavelength was usually 340 nm, unless otherwise specified. All optical measurements were performed at 23 $^{\circ}$C under ambient conditions. Samples for FTIR were prepared by mixing dry nanoparticles/hybrids powders in KBr and spectra were recorded in the diffused reflectance mode using IR Prestige-21 FTIR-8400s (Shimadzu Corporation, Japan) spectrometer.

For transmission electron microscopic (TEM) studies, samples were made on a carbon coated Cu grid through drop casting method. In order to avoid air oxidation of CdTe QDs[25-28] argon atmosphere was maintained throughout the experiment, including synthesis, self-assembly and sample preparation. Samples were removed from the inert atmosphere only at the time of TEM analysis. Specimens were imaged on a FEI's 300 kV high resolution **(FEI-**Tecnai G^2-30 with EDAX**)** transmission electron microscope. For XRD, samples were coated onto a pre-cleaned glass plate and data were acquired using a Panalytical PW 3040/60 X'Pert Pro powder diffractometer and Cu Kα1 radiation. Dynamic light scattering (DLS) and zeta potentials were measured using Zetasizer nanoseries (Zeta Nano–ZS, Ms. Malvern Instruments). A minimum of seven measurements for each sample were taken to ensure statistical significance. pH of the solution was monitored using Mettler Toldo (Five Go) pH meter.

Results and discussion

Synthesis of QDs: Synthesis and purification of water soluble CdTe nanoparticles having negative surface charges were accomplished by following the literature reports.[29, 30] In a typical procedure, sodium hydrogen telluride was freshly prepared by reducing tellurium powder (0.018 g, 0.14 mmol) with excess of sodium borohydride (0.35 g, 9.25 mmol) under argon atmosphere. Cadmium acetate dihydrate (0.078 g, 0.29 mmol) and thioglycolic acid (0.17 mL, 2.44 mmol) were taken in 125 mL doubly distilled water and pH of the solution was adjusted to 5.6 by adding aliquot amounts of 1 M sodium hydroxide. The reaction mixture was stirred under argon atmosphere for 20 min. To this, 5 mL of freshly prepared sodium hydrogen telluride solution was added and refluxed at ~100 $^{\circ}$C for 2.5 hours. Crystal growth was arrested by cooling the reaction mixture to room temperature. QDs thus obtained were purified by repeated precipitation from acetone, followed by centrifugation and finally re-dispersed in doubly distilled water. The zeta potential of the nanoparticles was varied through sequential removal of capping ligands by successive centrifugation (*vide infra*).

Similarly positively charged CdTe quantum dots (cysteamine stabilized) were prepared by adopting the method reported by X. Yang and co-workers.[30] Typically, 0.25 mL of 40 mM cadmium chloride, 0.25 mL of 0.1 M cysteamine, 0.25 mL of 10 mM sodium tellurite, 0.1 g of sodium borohydride and 5 mL of 1 M hydroxylamine hydrochloride were added to 15 mL of water such that the molar ratio between the reagent Cd^{2+}/TeO_3^{2-}/CA was maintained to be 4:1:10. After homogeneous mixing the solution was kept in water bath maintained at 40 $^{\circ}$C for 12 h.

Characterization: TEM and DLS analysis were employed to estimate the size and morphology of the synthesized nanoparticles. TEM images presented in Figure 1 showed that TGA capped nanoparticles (CdTe@TGA) has an average size of ~3 nm. The high resolution TEM images of the nanoparticles showed *d* spacing values of 0.35 ± 0.01 nm and 0.21 ± 0.01 nm which is characteristic of (111) and (220) lattice planes of CdTe(S) nanoparticles and confirms its zinc blende structure.[31, 32]More accurate values, 0.361 nm and 0.219 nm were obtained

from XRD measurements (Fig. 7). Whereas cysteamine capped nanoparticles (CdTe@CA) have relatively small sizes (~2.5). Similar observation was obtained from DLS analysis (Fig. S1 and S2).

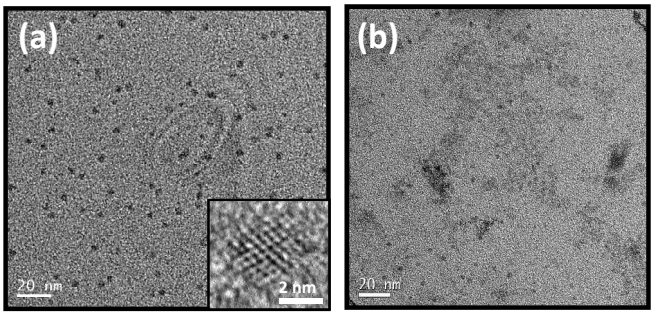

Figure 1. TEM images of (a) TGA and (b) CA capped CdTe nanoparticles.

Spectroscopic studies: Both the TGA and CA capped CdTe nanoparticles exhibit characteristic continuous absorption in the visible range (Fig. 2a). The first excitonic peak of CdTe@TGA nanoparticles is centred at ~ 530 nm and has an emission maximum around 560 nm which is in agreement with their measured size.[33] In accordance with their reduced size, CdTe@CA quantum dots show blue shifted absorption and emission profiles with maximum at ~ 495 nm and 530 nm respectively.

The organic counterparts, PMAH and PBA, have similar structured absorption and emission bands (Fig. 2a and 2b) that is unique of the pyrene core. For e.g., both the chromophores exhibit peaks corresponding to the I_1, I_2, I_3, I_4 and I_5 vibronic features of the fluorescence spectrum at ~374, 380, 385, 394 and 417 nm respectively. The I_3/I_1 ratio for both the molecules in water is estimated to be ~ 0.34 indicating that rather than the sign of appended chain, polarity of the surrounding has a great impact on their relative intensities (the value in cyclohexane is estimated to be 0.58 in Fig. S3). It has to be noted that the emission spectrum of both the pyrene chromophores are quite well separated from that of any of the nanoparticles used in the present study. This would allow the independent monitoring of the fluorescence signals of organic chromophores without having interference from that of QDs.

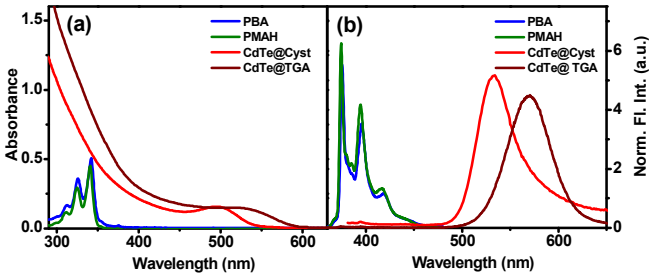

Figure 2. (a) Absorption and (b) Emission spectra in water of pyrene butyric acid (PBA, blue), pyrenemethylamine hydrochloride (PMAH, olive), cysteamine capped CdTe nanoparticles (red), thioglycolic acid capped nanoparticles (wine).

Surface charges: Earlier N. Gaponik et al. have shown that the surface charge of water soluble CdTe nanoparticles varies with type of protecting ligand and pH of the medium.[31] The zeta potential measurements of the present TGA and CA capped QDs resulted in surface charge values of ~ -46 mV and +21 mV respectively (Fig. 3). These measurements confirm that as intended the surface of respective nanoparticles are negative and positively charged. In the case of colloidal nanomaterials it is generally shown that their surface charge mainly originates from their capping ligands. Hence, we thought that zeta potentials can easily be modulated by their partial removal. In fact, nanoparticles having zeta values ~ -39, -35, and -31 mV were efficiently obtained by successive centrifugation (at 4000 rpm, 5 min) and are attributed to sequential removal of protecting ligands. It has to be noted that this treatment does not alter the size and morphology of the nanoparticles as is clearly evident from their similar absorption spectral profiles (Fig. 3b).

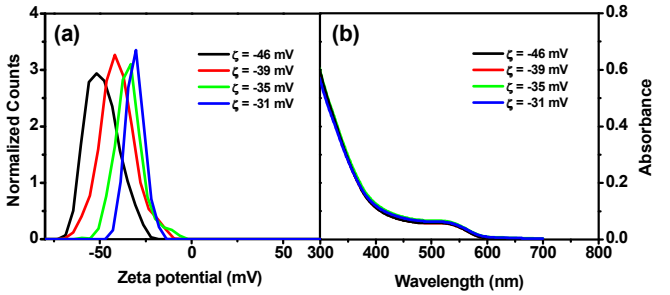

Figure 3. (a) Zeta potential curve and (b) corresponding absorption spectral profiles of CdTe@TGA quantum dots having different surface charges.

Binding studies: In order to study the electrostatically driven self-assembly between QDs and organic molecules, titration experiments were performed initially between CdTe nanoparticles and oppositely charged pyrene derivatives. Presented in Figure 4 are the absorption and emission spectral changes of PMAH in presence of increasing amounts of CdTe@TGA nanoparticles (ζ = -46 mV). The following can be easily noticed from the data. (i) An overall increase in the absorption profile from 200-600 nm. This is attributed to the continuous absorption of QDs in this range and whose magnitude increases with its concentration. (ii) The corresponding emission spectral measurements showed a continuous decrease in the PMAH fluorescence along with concomitant emergence of CdTe@TGA centred fluorescence. These spectral changes could be assigned to the combined effects of light partitioning, possibility of direct excitation of CdTe nanoparticles and the likely excited state energy transfer processes. However a detailed analysis of the data revealed that (i) the absorption profile of the mixture is exactly similar to that of algebraic sum of their individual contributions (inset of Fig. 4a). This suggests that the interaction of the chromophore with the nanoparticles does not bring any perturbation to electronic ground state of either of the two. Therefore it could also be argued that there is no change in the quantum confinement of individual CdTe nanoparticles upon self-assembly. On the other hand (ii) the emission profile of the PMAH in presence and

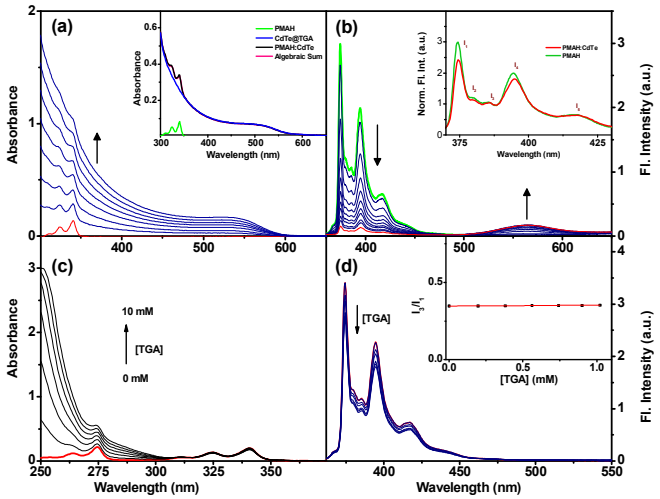

Figure 4. (a,c) Absorption and (b,d) emission spectral change of 2.5 μM PMAH in presence of increasing amounts of (a,b) CdTe@TGA having zeta -46 mV and (c,d) TGA; Inset shows (a) comparison of absorption spectra of PMAH (green), CdTe@TGA (blue), PMAH:CdTe@TGA (black) and algebraic sum (red), (b) normalized emission spectra of PMAH in the absence (green) and presence (red) of 1.8 μM CdTe@TGA (d) variation of I_3/I_1 value of PMAH in presence of TGA

absence of nanoparticles showed a clear difference in its I_3/I_1 fluorescence peak ratios (inset of Fig. 4b). An increase in the initial I_3/I_1 value of 0.34 to 0.45 has been observed in presence of 1.8 μM amounts of CdTe@TGA QDs. It is well established that the peak ratios of fluorescence vibronic features of pyrene increases with decrease in polarity of its immediate surroundings (*vide supra and Fig S3*). In the present case, compared to bulk medium (water, dielectric constant ~ 80), the surface of CdTe nanoparticles is expected to be less polar due to its low dielectric constant (~10) and presence of surface anchored hydrocarbons. Therefore when brought in close proximity of nanoparticles, through electrostatic interaction, the organic chromophore would experience less polarity, thus resulting in an increase in its I_3/I_1 ratio.

Due to their hydrophobic character, pyrene and other aromatic compounds are highly water insoluble. The improved solubility of the current derivative, PMAH (~2 mg in 10 mL), arises from the imparted hydrophilic character by the charged methylamine hydrocholoride appended part. Generally, electrostatic interaction between any two counterparts would lead to either a decrease in magnitude or complete neutralization of their charges. In the present case it could be expected that this process would eventually leads to an increase in hydrophobicity and subsequent precipitation. In fact, after a certain stages of titration, formation of agglomerates were visually observable in the cuvette (*vide infra*). In the case of such aggregates one could also argue that majority of the pyrene will be surrounded by similar molecules thus experiencing less polarity. This may also additionally contribute to the observed increase in I_3/I_1 ratio. Fortunately, in the case of pyrene, formation of such aggregates can easily be detected by its characteristic excimer emission at ~ 485 nm. However, throughout in our titration experiments we have never observed any such features in the emission spectrum thus ruling out the possibility of this contribution. Therefore the increase in I_3/I_1 ratio could only be attributed to the vicinity of the chromophore to the nanoparticle surface via electrostatic interaction. This was further confirmed by our titration experiments with high concentration of PMAH (but just below its critical concentration for excimer formation ~ 40 μM) where addition of nanoparticles resulted in immediate formation of large agglomerates. Even in such cases the fluorescence spectrum didn't show any features corresponding to excimer formation.

Further efforts were devoted to probe the self-assembly via other spectroscopic measurements. However, the inevitable immediate precipitation of assembly at higher concentrations, i.e. required for NMR studies, (Fig S4) hindered us in making any conclusive interpretations. Therefore, attempts were further made to characterize the nanohybrids via FTIR technique (Fig. 5). The characteristic S–H vibrations band (at 2570 cm^{-1}) were absent in the IR spectrum of CdTe@TGA QDs indicating the anchoring of TGA molecules through S atom.[34, 35] As reported by others, compared to free molecule, the asymmetric stretching vibration of the carboxylate groups of TGA on CdTe nanoparticles appeared at lower frequencies around 1570 cm^{-1}. A further lowering of this vibrational energy to ~1550 cm^{-1} was observed in the case of hybrids indicating the electrostatic interaction.

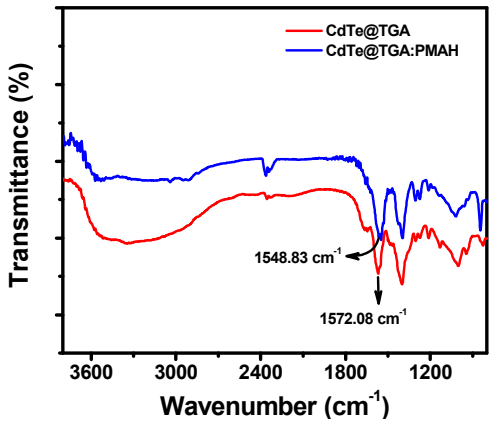

Figure 5. FTIR spectra of CdTe@TGA nanoparticles and CdTe@TGA:PMAH hybrid.

Role of nanoparticle and its surface charge

In order to further prove the necessity of nanoparticle, its surface charge and hence the role of electrostatic interaction, we have carried out several experiments and the results are described below.

(i) Role of Nanoparticles: So as to invoke this, titration experiments were performed with PMAH and the capping ligand TGA under identical conditions. In presence of very low concentrations (micro molar) of TGA, no considerable absorption or emission spectral changes were observed. At higher concentrations (above 1 mM), there was a continuous increase in absorbance below 300 nm arising from the

contribution of TGA (Fig. 4c, Fig. S5). However both the absorbance at longer wavelengths and the relative intensities of I_1 and I_3 peaks (Fig. 4d) remain unaltered. This indicates that the presence of nanoparticles is highly essential for the observed Ham effect.

(ii) The role of surface charges.

(a) Zeta potential measurements: It is well known that the stability of colloidal solutions arises from their surface charges. The strong electrostatic repulsion between the particles prevents them from aggregation. As described in before, if the interaction of CdTe@TGA QDs with PMAH is electrostatic in nature, then there will be a decrease in magnitude of surface charge. In order to investigate this aspect zeta potentials of nanoparticles were monitored in presence of varying PMAH concentrations. With increase in its concentration, an almost linear decrease in zeta value of nanoparticle to around -20 mV was observed (Fig. 6a). A further increase in its concentration resulted in a sudden drop in zeta value around -8 mV and precipitation of QDs.

(b) Interaction with QDs having different surface charges: Further to understand the effect of magnitude of electric charge on the electrostatic interaction, titration experiments were performed by adding fixed amounts of nanoparticles (same optical density) having different surface charges into 2.5 μM solution of PMAH (Fig. 6b and S6). Earlier W. W. Yu *et al.* has shown that the extinction coefficient of CdTe nanoparticles are independent of their preparation conditions.[36] Therefore the concentration of nanoparticles is ensured to be the same in all samples by adjusting its OD at ~ 530 nm to be 0.22. It has been noted that, for a particular concentration ratio, the magnitude of I_3/I_1 value is highly proportional to the surface charge of nanoparticles (Fig. 6b). For example, QDs having a high zeta value of -46 mV showed the highest I_3/I_1 value of 0.54 and that having -20 mV showed a lowest value of 0.41. Our attempts to study the electrostatic interaction of nanoparticles having further low zeta values were limited by the instability of solution.

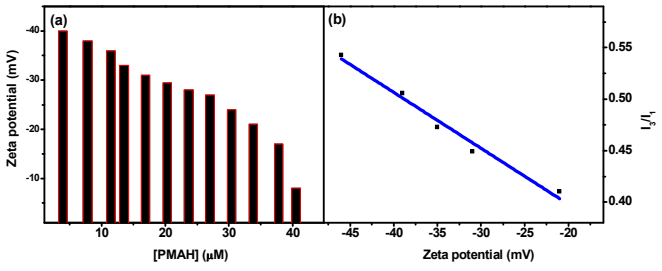

Figure 6. Variation of (a) zeta potential of the nanoparticles in presence of increasing amounts of PMAH and (b) I_3/I_1 ratios of PMAH in presence of nanoparticle having varying surface charges.

(c) Interaction of positively charged QDs: Similar titration experiments were performed using cysteamine capped CdTe nanoparticles (ζ = + 21 mV) and pyrene butyric acid (Fig. S7a). As expected, in the presence of nanoparticles, an increase in the I_3/I_1 ratio was noted indicating the occurrence of electrostatic interaction. On the contrary, no change in I_3/I_1 value was observed when positively charged nanoparticles were titrated with pyrene chromophore having similar charge, PMAH (Fig. S7b). These experiments clearly demonstrate that the organic chromophore is brought in close proximity of nanoparticle through electrostatic interaction which in turn results in Ham effect.

Morphological Characterization of Nanohybrids

As it was clear that the electrostatic interaction leads neutralization of charges and subsequent precipitation (*vide supra*), efforts were paid to characterize the morphology of the resulting nanohybrids through TEM analysis. The low magnification images revealed the presence of several nano-micro scale objects having different morphologies, mostly sheet like structures (Figure 7 and S8). Whereas no such features were visible in the TEM grid containing CdTe@TGA QDs alone. At higher magnifications, it has been found that these nano/microstructures are composed of nanoparticles having size ~ 3 nm. Even though there were no regular patterns of organization for these nanoparticles, areas with single hexagonal close packing were identified. It has to be specifically noted that the identity of the QDs are maintained in these agglomerates. In particular, the crystalline structures of individual particles are well preserved as is clear from the HRTEM images. Thus maintaining the same quantum confinement of QDs as same as before their agglomeration. This aspect was also evident in the absorption and emission spectral studies (Fig 4.). Even at the end of the titration there was no red-shift to excitonic band of the QDs. However, a small bathochromic shift of maximum ~ 5 nm (Fig. S9) has been noticed in the emission spectrum of nanoparticles and could only be attributed to the possible energy migration between the QDs in the assembly.[27, 37] These findings were further supported by XRD measurements (Fig 7e). The XRD of the nanohybrids are quite similar with that of the initial nanoparticles illustrating the same crystallinity as before self-assembly. The FWHM of the signal was negligibly affected revealing that there is no change in the nanoparticles grain size.

Organization of QDs into higher order assemblies is essential for their practical utilization in optoelectronic and photonic devices.[38, 39] There have been both covalent and non-covalent efforts to realize such nano and micro scale assemblies mainly through bottom-up strategies. One of the major challenges is to obtain superstructures without fusing of the precursor nanocrystals and preserving their initial quantum confinement and properties. In one of the earlier works, Z. Tang and coworkers reported that 2-(Dimethylamino)ethanethiol (DMAET) capped CdTe and CdSe QDs with positive zeta potentials self-assemble in water to form free floating sheets and are composed of monolayers of NPs assembled in 2D network fashion.[40] Anisotropic electrostatic interactions and directional hydrophobic attractions were the main driving force for the formation of such 2D free-floating films. Similarly, assembly of CdTe QDs

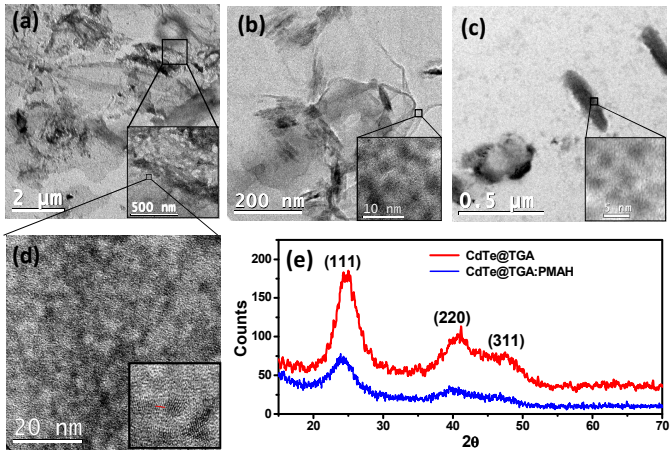

Figure 7. (a-d) TEM images of the nanohybrids formed via electrostatic interaction; insets shows the higher magnification images from selected areas (e) XRD spectra of CdTe@TGA and CdTe@TGA:PMAH hybrid.

into nanowire networks were obtained upon screening their surface charge by ions in the buffer.[37] The other approach include reduction of ligand surface density by the addition of organic solvents thus weakening the charge-charge repulsion and which fosters attractive dipole-dipole, van der Waals and hydrogen bonding interactions.[41] Though we used methanol (to prepare stock solution of PMAH), its percentage is only < 0.2 % in the current studies and is insufficient to cause any destabilization of the ligand shell. It could also be argued that PMAH may directly bind with nanocrystal surface by replacing the bound ligands and thus resulting in changes surface charges. However, the control experiments with positively charged nanoparticles disprove this point (*vide supra* and Fig. S7). In the current studies, the strong electrostatic repulsion due to high surface charge (ζ = -46 mV, imparted by the carboxylate group of the thioglycolic acid) is the main reason that prevents the nanoparticles from agglomeration. Upon interaction with the oppositely charged organic chromophores there is a dramatic decrease in the zeta potential (Fig. 6a) thus reducing the magnitude of interparticle Coulumbic repulsion. Along with this, the vicinity of PMAH to the nanoparticle surface and its neutralization of the charges in turn cause an overall raise in the hyrdophobicity of the system. These two complementary, yet favoring phenomena trigger the self-assembly process. These arguments were further supported by the DLS measurements. Along with decrease in zeta potential there was a gradual raise in the aggregate size (Fig. S10) with increase in PMAH concentration. Formation of mainly two-dimensional sheets suggest that after the diminishing of charge-charge repulsion the self-assembly is fostered through long range dipole-dipole and hydrophobic interactions as is observed by Tang et al.[40]

Conclusions

In summary, a series of water soluble cadmium telluride nanoparticle having different zeta potentials were synthesized. We have shown that the polarity difference between the bulk medium and nanoparticle surfaces can be effectively utilized to study their interaction with organic chromophores. In short, there was an increase in I_3/I_1 value (Ham effect) upon self-assembly. However no change in I_3/I_1 ratio was detected in presence of capping ligand alone. Even its value remains unaltered when pyrene molecules interact with similarly charged QDs. Moreover the magnitude of Ham effect linearly increases with zeta potential of nanoparticles. These observations conclusively support the role of QDs and its surface charge in the self-assembly process and hence Ham effect. Furthermore, we observed that the initial electrostatic interaction between organic and inorganic counter parts results in neutralization of their surface charges. Together with this, the raise in hydrophobicity induces their further organization into macroscale sheet like structures. Therefore, these studies bestow a clear insight that controlled modulation of the surface charges and solvophobicity could be a versatile methodology to generate superstructures of nanocrystals which preserves their initial quantum confinement. Such higher order assemblies of nanocrystals could be an ideal platform for developing light emitting devices and solar cells. As thioglycolic acid stabilized CdTe QDs are known to undergo easy oxidation, extending this strategy with more stable nanoparticles and their utilization as active material in optoelectronic devices is presently under progress in the lab.

Acknowledgements

This work is financially supported by CSIR's network projects Molecules to Materials to Devices (CSC-0134) and TAPSUN (NWP0054). Authors acknowledge the expert assistance of Mr. Robert Philip and Mr. Kiran Mohan for recording the transmission electron microscopic images.

Notes and references

[a] Photosciences and Photonics Section, Chemical Sciences and Technology Division, CSIR-National Institute for Interdisciplinary Science and Technology, Thiruvananthapuram 695019, Kerala, India. email: yoosafk@niist.res.in

[b] Academy of Scientific and Innovative Research (AcSIR), New Delhi 110001, India.

Electronic Supplementary Information (ESI) available: [additional absorption and emission spectra, DLS, zeta potential data and TEM images of the organic molecules, nanoparticles and self-assembled systems]. See DOI: 10.1039/b000000x/

1. C. Sanchez, B. Julian, P. Belleville and M. Popall, *J. Mater. Chem.*, 2005, **15**, 3559-3592.
2. E. Holder, N. Tessler and A. L. Rogach, *J. Mater. Chem.*, 2008, **18**, 1064-1078.
3. Y. Zhou, M. Eck and M. Kruger, *Energy Environ. Sci.*, 2010, **3**, 1851-1864.
4. X. Fan, M. Zhang, X. Wang, F. Yang and X. Meng, *J. Mater. Chem. A*, 2013, **1**, 8694-8709.
5. V. L. Colvin, M. C. Schlamp and A. P. Alivisatos, *Nature*, 1994, **370**, 354-357.

6. Y. Shirasaki, G. J. Supran, M. G. Bawendi and V. Bulovic, *Nat. Photon*, 2013, **7**, 13-23.
7. V. Biju, T. Itoh and M. Ishikawa, *Chem. Soc. Rev.*, 2010, **39**, 3031-3056.
8. Y. Hu, D. H. Fine, E. Tasciotti, A. Bouamrani and M. Ferrari, *Wiley Interdiscip. Rev. Nanomed. Nanobiotechnol.*, 2011, **3**, 11-32.
9. N. Erathodiyil and J. Y. Ying, *Acc. Chem. Res.*, 2011, **44**, 925-935.
10. L. Nicole, L. Rozes and C. Sanchez, *Adv. Mater.*, 2010, **22**, 3208-3214.
11. H. Wei, S. Du, Y. Liu, H. Zhao, C. Chen, Z. Li, J. Lin, Y. Zhang, J. Zhang and X. Wan, *Chem. Commun.*, 2014, **50**, 1447-1450.
12. T. Yoon, J. Kim, J. Kim and J. Lee, *Energies*, 2013, **6**, 4830-4840.
13. D. M. Guldi, G. M. A. Rahman, V. Sgobba, N. A. Kotov, D. Bonifazi and M. Prato, *J. Am. Chem. Soc.*, 2006, **128**, 2315-2323.
14. S. C. Olugebefola, A. R. Hamilton, D. J. Fairfield, N. R. Sottos and S. R. White, *Soft Matter*, 2014, **10**, 544-548.
15. S. M. Oliveira, T. H. Silva, R. L. Reis and J. F. Mano, *Adv. Healthcare Mater.*, 2013, **2**, 422-427.
16. E. Vaishnavi and R. Renganathan, *Analyst*, 2014, **139**, 225-234.
17. D. Savateeva, D. Melnikau, V. Lesnyak, N. Gaponik and Y. P. Rakovich, *J. Mater. Chem.*, 2012, **22**, 10816-10820.
18. K. Kalyanasundaram and J. K. Thomas, *J. Am. Chem. Soc.*, 1977, **99**, 2039-2044.
19. D. C. Dong and M. A. Winnik, *Photochem. Photobiol.*, 1982, **35**, 17-21.
20. D. C. Dong and M. A. Winnik, *Can. J. Chem.*, 1984, **62**, 2560-2565.
21. E. Villemin, B. Elias, M. Devillers and J. Marchand-Brynaert, *Molecules*, 2013, **18**, 1897-1915.
22. N. Idayu Zahid, O. K. Abou-Zied, R. Hashim and T. Heidelberg, *J. Phys. Chem. C*, 2011, **115**, 19805-19810.
23. B. Itty Ipe, K. Yoosaf and K. G. Thomas, *Pramana - J. Phys.*, 2005, **65**, 909-915.
24. D. M. Sena Jr, H. O. Pastore and F. B. T. Pessine, *Phys. Chem. Chem. Phys.*, 2009, **11**, 7219-7224.
25. D. Deng, L. Qu, Y. Li and Y. Gu, *Langmuir*, 2013, **29**, 10907-10914.
26. Z. Tang, N. A. Kotov and M. Giersig, *Science*, 2002, **297**, 237-240.
27. H. Chen, V. Lesnyak, N. C. Bigall, N. Gaponik and A. Eychmüller, *Chem. Mater.*, 2010, **22**, 2309-2314.
28. Z. Tang, Y. Wang, K. Sun and N. A. Kotov, *Adv. Mater.*, 2005, **17**, 358-363.
29. P. V. Nair and K. G. Thomas, *J. Phys. Chem. Lett.*, 2010, **1**, 2094-2098.
30. J. Pei, H. Zhu, X. Wang, H. Zhang and X. Yang, *Anal. Chim. Acta*, 2012, **757**, 63-68.
31. N. Gaponik, D. V. Talapin, A. L. Rogach, K. Hoppe, E. V. Shevchenko, A. Kornowski, A. Eychmüller and H. Weller, *J. Phys. Chem. B*, 2002, **106**, 7177-7185.
32. A. L. Rogach, *Mater. Sci. Eng., B*, 2000, **69–70**, 435-440.
33. A. Mandal and N. Tamai, *J. Phys. Chem. C*, 2008, **112**, 8244-8250.
34. L. Li, Y. Cheng, Y. Ding, S. Gu, F. Zhang and W. Yu, *Eur. J. Inorg. Chem.*, 2013, **2013**, 2564-2570.
35. Y. Wang, J. Lu, Z. Tong, B. Li and L. Zhou, *Bull. Chem. Soc. Ethiop.*, 2011, **25**, 393-398.
36. W. W. Yu, L. Qu, W. Guo and X. Peng, *Chem. Mater.*, 2003, **15**, 2854-2860.
37. Y. P. Rakovich, Y. Volkov, S. Sapra, A. S. Susha, M. Döblinger, J. F. Donegan and A. L. Rogach, *J. Phys. Chem. C*, 2007, **111**, 18927-18931.
38. D. Zhou, M. Liu, M. Lin, X. Bu, X. Luo, H. Zhang and B. Yang, *ACS Nano*, 2014, **8**, 10569-10581.
39. A. S. Baimuratov, I. D. Rukhlenko, V. K. Turkov, A. V. Baranov and A. V. Fedorov, *Sci. Rep.*, 2013, **3**, 1727.
40. Z. Tang, Z. Zhang, Y. Wang, S. C. Glotzer and N. A. Kotov, *Science*, 2006, **314**, 274-278.
41. F. Jiang and A. J. Muscat, *J. Phys. Chem. C*, 2013, **117**, 22069-22078.

Graphical Abstract

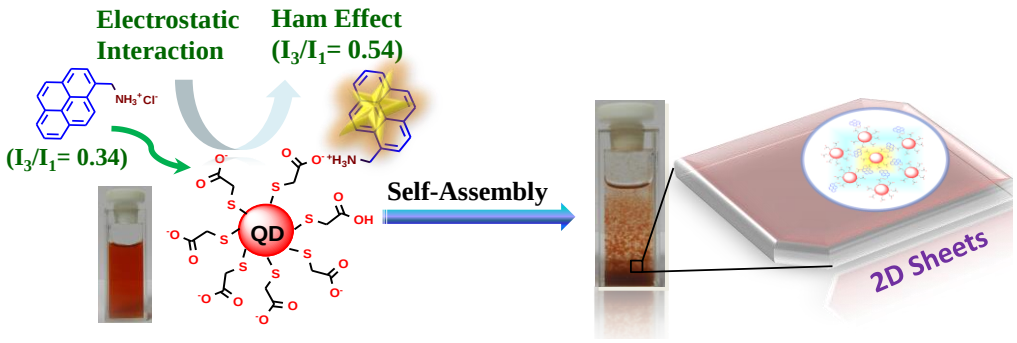

The polarity difference between nanoparticle surface and medium is utilized for studying electrostatically driven self-assembly; Diminishing of the repulsive forces via charge neutralization fosters the self-organization of QDs into 2D sheets.